From ±120 kV BTB HVDC Experience to the Design of a ±525 kV 2 GW GFM HVDC System for Korea's West-Coast Energy Highway

Jun-chol Lee
Hyosung Corporation, Seoul, Republic of Korea
Yonsei University
Seoul, South Korea
juniwas@hyosung.com

Minsung Kim and Kyeon Hur
School of Electrical and Electronic Engineering
Yonsei University
Seoul, South Korea
alstjd0621@yonsei.ac.kr, khur@yonsei.ac.kr

***Abstract*—South Korea is currently addressing a critical geographic imbalance between its primary renewable generation base in the southwestern Honam region and the high-density load centers of the Seoul Metropolitan Area (SMA). This mismatch has induced chronic transmission congestion and pushed metropolitan short-circuit levels toward the breaking limits of existing infrastructure. To mitigate these operational bottlenecks, the ±120 kV 200 MW Yangju back-to-back (BTB) voltage-source converter (VSC) system—Korea's inaugural MMC-HVDC installation—was successfully operationalized to perform bus sectionalization, effectively decoupling fault-current contribution paths while maintaining bidirectional flexibility. Building upon this foundation, the 'Seohaean Energy Highway' initiative has been launched to establish a ±525 kV 2 GW MMC-HVDC backbone for bulk power transfer from the renewable-concentrated south to the SMA. To safeguard stability against declining short-circuit ratios (SCR) in the southwestern grid and manage stringent network configurations in Seoul, the proposed system integrates advanced grid-forming (GFM) control. This paper presents the Yangju operational results, the 2 GW system architecture, and simulation-based verification of GFM performance under weak-grid and high-density load conditions.**

***Index Terms*—GFM, HVDC, MMC, Power System Stability, Renewable energy transmission**

I. Introduction

The rapid expansion of renewable generation in South Korea's southwestern Honam region, combined with the high load density of the Seoul metropolitan area (SMA), has created a pronounced regional supply-demand imbalance. This divergence results in severe transmission congestion and pushes short-circuit currents toward the breaking limits of existing infrastructure. While traditional High-Voltage AC reinforcement could theoretically facilitate power transfer, constructing new AC corridors has become prohibitively challenging due to limited land availability and significant public opposition to overhead pylons. To address these operational bottlenecks, the ±120 kV, 200 MW Yangju back-to-back (BTB) system was operationalized in 2024 as Korea's first MMC-based VSC-HVDC installation. This project provided a tactical solution through bus sectionalization, effectively decoupling fault-current contribution paths to ensure the fault-interrupting capability of existing 154 kV circuit breakers. Beyond fault mitigation, the system enhances reliability through controllable active power redistribution and transient voltage support via dynamic reactive power control. Building upon this proven foundation, the Korean government has launched the Seohaean Energy Highway initiative. This national project involves developing a ±525 kV, 2 GW bipole MMC-HVDC backbone to reliably transmit renewable power from the south to the SMA. As the Honam grid faces declining short-circuit ratios (SCR) and reduced natural inertia, the proposed system integrates advanced grid-forming (GFM) control [1]. To ensure multi-vendor compatibility and robust performance, the GFM functionality is designed and verified against the InterOPERA (Interoperability and Operation of HVDC Grids with Renewable Energy Sources) framework. This paper outlines the operational results from the Yangju BTB project, the development plan for the ±525 kV 2 GW system, and simulation-based verification of GFM control following the InterOPERA functional requirements [2].

(Corresponding Author: Kyeon Hur.)

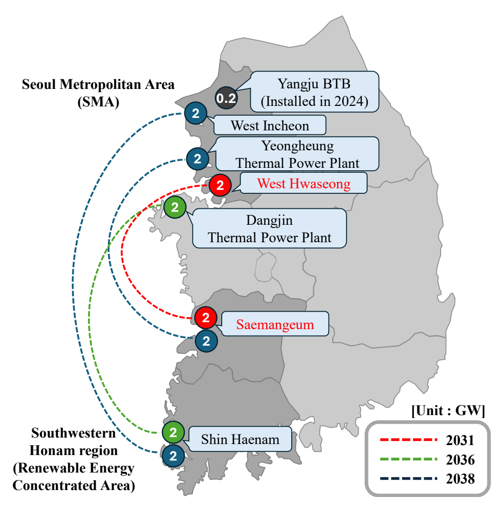

Fig. 1. Seohaean Energy Highway roadmap outlined in the 11th Basic Plan for Long-Term Electricity Supply and Demand in Korea [3].

979-8-3315-8138-1

II. YANGJU ±120 KV 200 MW MMC-HVDC PROJECT

A. Background

The ±120 kV, 200 MW Yangju BTB MMC-HVDC system was installed to mitigate high fault currents and transmission congestion in the northern metropolitan power grid. The system enhances the network's overall performance by reducing fault current, mitigating line overloading, and improving voltage stability through dynamic reactive-power control, while also increasing system reliability and operational flexibility through controllable power flow.

1) Grid Segmentation Effect of the BTB HVDC System: When the BTB HVDC system is applied, the AC network is electrically isolated by the converter, thereby reducing fault current. Table I compares the fault currents in SMA with and without the BTB HVDC system. The BTB system was installed at the originally unified Bus 1410 to sectionalize the high-fault current node into two separate buses: 1410 and 1411. This configuration electrically decouples the AC networks and splits the fault-current contribution paths. As shown, the BTB HVDC system reduces the fault current to below 50 kA, ensuring the fault-interrupting capability of 154 kV circuit breakers.

TABLE I
FAULT CURRENT WITH AND WITHOUT BTB MMC–HVDC

Bus number	Base kV	Fault Current [kA]	
		With BTB	Without BTB
1400	345	48.2340	50.1957
1310	154	47.8011	48.3293
1410	154	49.7672	65.5842
1411	154	25.7956	65.5842
1435	154	44.3816	49.5401
1454	154	46.0151	47.7584
1470	154	43.6589	49.6409
1475	154	46.1315	51.8724
1490	154	46.2564	52.0078
1810	154	48.2441	53.2228
1811	154	47.7596	52.6257

2) System overload Improvement using Power flow control: The BTB MMC-HVDC system provides direct controllability of active power. Adjusting power flow in neighboring areas can redistribute power when a specific line becomes overloaded. Fig. 2 shows how BTB power control mitigates line overload during a contingency event [4].

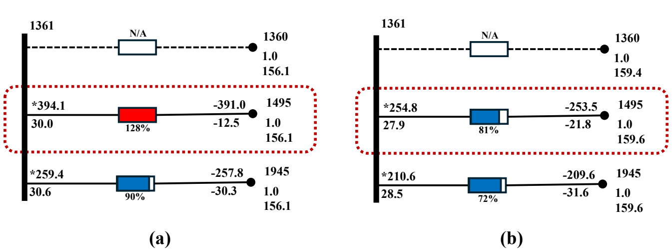

Fig. 2. Overload comparison. (a) Without BTB MMC-HVDC (b) With BTB MMC-HVDC

3) Transient voltage support using reactive power control: The BTB MMC-HVDC supports voltage compensation by supplying reactive power under low-voltage conditions in the AC grid, thereby improving voltage stability. Fig. 3 compares voltages with and without BTB during a fault near the 154 kV system in Yangju. The BTB compensates the voltage by supplying about 60 MVar of reactive power, raising it by approximately 0.05 pu.

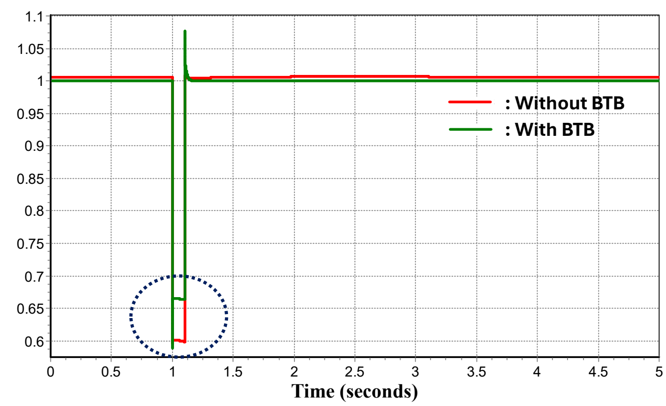

Fig. 3. Transient voltage comparison Without and With BTB MMC-HVDC.

B. System Configuration, Control, and Commissioning Performance of the Yangju HVDC System

1) Overall System Configuration and Converter Station: The Yangju ±120 kV 200 MW BTB HVDC system adopts a symmetrical-monopole configuration based on the MMC topology as shown in Fig. 4. Each converter station is connected to the 154 kV metropolitan AC grid through coupling transformers rated at 213.6 MVA (154 kV/127.7 kV). The specifications of the system are summarized in Table II. Power exchange between the two AC systems is managed through coordinated converter controls, including DC-voltage regulation and active-power control, ensuring stable and flexible operation under varying system conditions. Each converter comprises six arms, and each arm consists of 108 submodules (SMs) rated at DC 2.4 kV, including 8 redundant SMs. This configuration enables stepwise voltage synthesis and low harmonic distortion. The MMC topology significantly reduces the need for large AC filters and enhances operational efficiency and reliability [5]. To minimize the overall station footprint, the converter building was designed with an optimized layout that efficiently arranges the converter room, DC switch room, and cooling facilities within the site boundary.

TABLE II
MAIN SPECIFICATIONS OF YANGJU BTB HVDC SYSTEM

Contents		Description
Station	Size	203.4' (W) × 167.3' (D) × 55.8' (H)
	Rated Capacity	200 MW, ±120 kVDC
Converter TR.		213.6 MVA, 154 kV / 127.7 kV
Sub-Module	Rated Voltage	2.4 kVDC
	Num./Arm	108

979-8-3315-8138-1

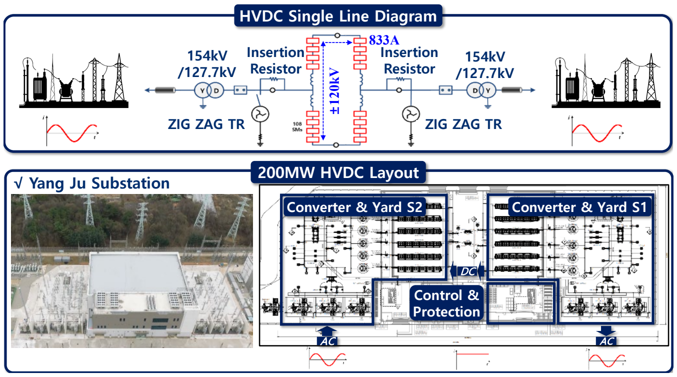

Fig. 4. Overall Yangju BTB HVDC System Configuration.

The Yangju HVDC station also employs a fully redundant digital control and protection (C&P) architecture composed of Operating, control, and AC Protection systems. The Operating system integrates operator/engineering workstations, servers, and GPS-based time synchronization. The Control system, including the Converter Control & Protection (CCP) and ARM controllers, manages power and voltage control, converter protection, modulation, and submodule voltage balancing. The AC Protection system uses protection IEDs and bay controllers for transformer, busbar, and switchgear protection. All controllers are interconnected via a redundant IEC 61850-based LAN, ensuring high system availability and fault tolerance.

2) Commissioning and Performance validation: Comprehensive commissioning tests were conducted to validate the dynamic performance and operational stability of the Yangju HVDC system. The commissioning and performance validation program included a wide range of tests such as active/reactive power response tests, redundancy switchover tests, protection operation tests, power quality measurements, heat run tests, and operation and integration tests. Among these, the specifications and representative results of three key response tests are summarized below.

- Active-Power Response Test: The system responded within 200 ms to a ±1 p.u. step change in active-power reference, demonstrating fast transient control capability and stable power regulation, as shown in Fig. 5(a).
- Reactive-Power Response Test: The converter reacted within one cycle ($\approx$ 16.6 ms) to a ±1 p.u. step change in reactive power, confirming rapid voltage recovery and transient voltage stabilization at the PCC, as shown in Fig. 5(b).
- Run-up/Run-back/Fast Runback Tests: The controller dynamically adjusted power according to 20 predefined command signals transmitted from the Remote-Control Center. The Fast Runback Test, in particular, was conducted to validate compliance with the specified performance requirement achieving power reduction within 100 ms and maintaining stable operation for more than 140 ms after runback initiation, as illustrated in Fig. 6.

The results confirmed that the Yangju HVDC control and protection system provides fast dynamic response, reliable AC protection coordination, and stable operation under steady-state and transient grid conditions.

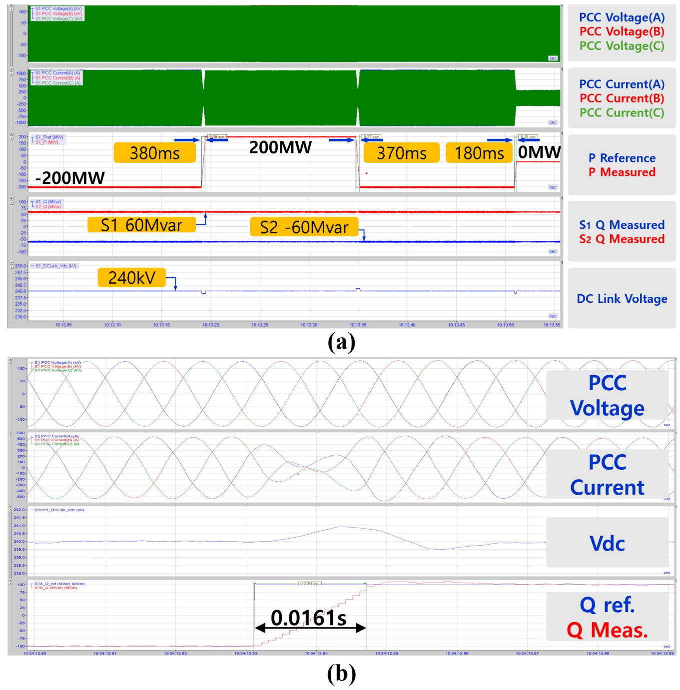

Fig. 5. Yangju HVDC system Performance Validation. (a) Active-Power Response, (b) Reactive-Power Response

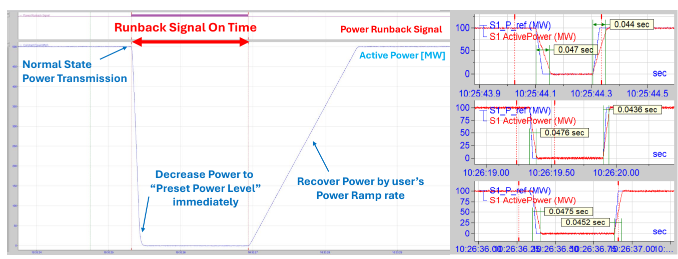

Fig. 6. Power Run-back/up/Fast Runback Performance Test Results

III. DEVELOPMENT OF THE ±525 KV 2 GW BI-POLE HVDC

A. National Program and Project Development

The Korean government has established the Seohaean Energy Highway Initiative as part of the 11th Basic Plan for Long-Term Electricity Supply and Demand (2024–2038), a 15-year national roadmap aimed at addressing the growing imbalance between renewable generation in coastal regions and electricity demand in SMA. This initiative comprises four ±525 kV 2 GW bi-pole MMC-HVDC systems along the west coast, designed to transmit renewable power generated from large-scale offshore wind and photovoltaic clusters directly to major load centers such as Seoul and Incheon. Among these, the Saemangeum–Seohwaseong HVDC link, the first project of the program, was originally scheduled to start in 2031. However, due to the strategic importance of the project,

979-8-3315-8138-1

the government is planning to advance the target completion year to 2030, signaling its strong commitment to accelerate HVDC system deployment in support of the national energy transition. In alignment with this policy direction, Hyosung Heavy Industries is advancing the development of a ±525 kV 2 GW bi-pole HVDC system based on the proven technologies and successful design and operational experience gained from the Yangju ±120 kV 200 MW BTB MMC-HVDC demonstration project. Building upon this foundation, Hyosung Heavy Industries has launched a large-scale R&D program targeting completion by 2027, focusing on the development of high-voltage and high-capacity converter valves, bi-pole converter transformers, and an integrated control and protection (C&P) system optimized for large-scale applications. Particular emphasis has been placed on ensuring system stability at the Saemangeum sending-end station, where the local short-circuit ratio (SCR) is expected to be weak due to the high penetration of renewable generation. To address these grid conditions, Hyosung has developed a GFM-based bi-pole HVDC simulation model that satisfies all 12 interoperability functions defined in the InterOPERA GFM HVDC framework [2]. This simulation platform incorporates advanced control algorithms and interoperability features required for future multi-terminal and multi-vendor HVDC networks, ensuring that the 2 GW system can provide not only power transfer but also grid-supporting functionalities such as self-synchronization, inertial response, and voltage regulation.

B. GFM-Based Bi-pole HVDC Simulation Model and Functionality

The developed GFM-based ±525 kV bi-pole HVDC simulation model follows the functional requirements outlined by NERC [6] and InterOPERA, designed to ensure autonomous operation, self-synchronization, and system inertia support under weak grid conditions. Among the various control strategies for grid-forming converters [7], Hyosung implemented two representative methods(Droop Control and Virtual Synchronous Machine (VSM) Control). According to the NERC definition, grid-forming control maintains an internal voltage phasor that remains constant (or nearly constant) during transient disturbances, allowing the inverter to behave as a voltage source capable of providing inertia and reactive support. The implemented controllers operate as follows:

- Droop Control: Adjusts the converter frequency and voltage setpoints according to the measured active and reactive power deviations (P–f and Q–V droop).
- VSM Control: Emulates the swing equation of a synchronous generator to provide inertial response and damping under grid disturbances.

Fig. 7 illustrates the PSCAD-based simulation environment established to verify the grid-forming functionalities. The environment includes a two-station configuration (Station 1: GFL mode with DC-voltage control, Station 2: GFM mode), GFM control parameters (Droop and VSM settings), and test cases defined in accordance with the InterOPERA framework. It also covers a range of SCRs and X/R ratios representative of weak-grid conditions, along with the operating modes and reference set-points required for each test item. Under this environment, the developed GFM-based ±525 kV bi-pole HVDC model was tested against InterOPERA's 12 functional requirements, and the system successfully satisfied all performance criteria across all test items.

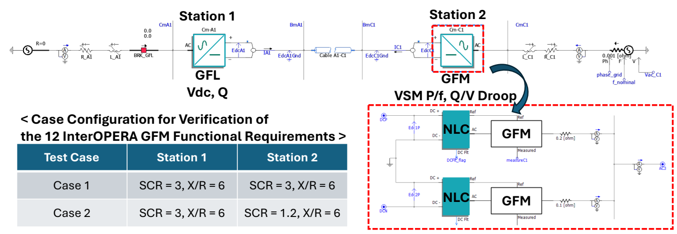

Fig. 7. PSCAD Simulation model for InterOPERA 12 GFM Functional Requirements Verification

TABLE III
PSCAD SIMULATION MODEL PARAMETERS

Parameter	Value	Parameter	Value
dt (Solution time step, μs)	10	I_{lim} (Current limit, pu)	1.2
$K_{p,c}$ (Current control P)	0.5	$K_{i,c}$ (Current control I)	20
$K_{p,v}$ (Voltage control P)	3	$K_{i,v}$ (Voltage control I)	400
m_p (P–f droop ratio)	0.05	m_q (Q–V droop ratio)	0.03
D (VSM damping)	20	J (VSM inertia, s)	1

Among the 12 GFM functionalities defined in the InterOPERA framework, two representative functions (Phase Jump Active Power, Inertial Active Power) were selected to demonstrate the verification methodology and transient performance of the developed ±525 kV 2 GW bi-pole HVDC system. The following subsections describe each function, theoretical background, and PSCAD-based simulation results.

1) Phase Jump Active Power: This function evaluates the converter's capability to provide rapid and proportional active-power support when a sudden grid phase-angle disturbance ($\Delta\delta$) occurs, such as during network switching or fault recovery. The converter must maintain synchronization and suppress transient oscillations through autonomous control.

As shown in Fig. 8, two representative GFM control modes (Droop and VSM) were compared under ±5° phase-jump conditions. Both control modes satisfied the InterOPERA GFM capability requirements, but they exhibited distinct transient characteristics. The Droop controller regulated active power proportionally to steady-state deviation, enabling smooth recovery without inertia. In contrast, the VSM controller, based on the swing equation of a synchronous generator, provided an instantaneous active power burst proportional to the rate of phase change (RoCoF), yielding superior inertial response and oscillation damping. Consequently, the VSM-based control showed better stability and robustness under weak-grid conditions, making it particularly suitable for the Saemangeum sending-end station of the Seohaean Energy Highway project.

2) Inertial Active Power: This function assesses the converter's capability to provide additional active power proportional to the rate of change of frequency (RoCoF), contributing

979-8-3315-8138-1

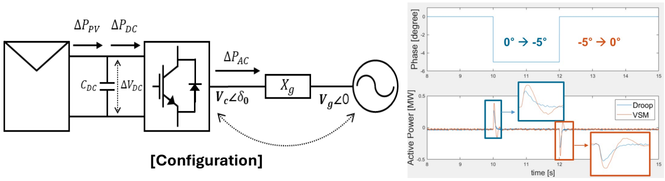

Fig. 8. Simulation results of droop and VSM control under ±5° phase-jump condition, showing phase angle and active-power response.

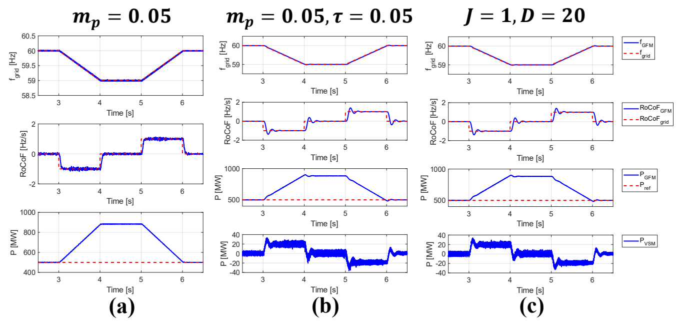

Fig. 9. Frequency responses of the GFM HVDC converter. (a) Droop, (b) Droop + LPF, and (c) VSM control modes.

to virtual inertia and frequency stabilization. Based on this principle, three representative GFM control methods (Droop Control, Droop with Low-Pass Filter (LPF), and VSM Control) were implemented for comparison. The corresponding mathematical formulations are as follows [8]:

$$\omega_{\text{droop}} = m_p \left(P_{\text{ref}} - P_m\right) + \omega_0 \tag{1}$$

$$\omega_{\text{droop+LPF}} = m_p \left(\frac{1}{\tau s + 1}\right) \left(P_{\text{ref}} - P_m\right) + \omega_0 \tag{2}$$

$$J \frac{d\omega_{\text{VSM}}}{dt} = P_{\text{ref}} - P_m - D\left(\omega_{\text{VSM}} - \omega_0\right) \tag{3}$$

where m_p is the active-power droop coefficient, τ is the LPF time constant, J is the inertia constant, and D is the damping factor.

As illustrated in Fig. 9, the conventional droop controller provides the active-power output in proportion to the frequency deviation Δf, i.e., it provides a steady-state power response to a frequency drop but does not inherently generate an inertial response proportional to RoCoF. In contrast, the VSM control emulates the synchronous-generator swing equation and therefore produces an inertial active-power component proportional to RoCoF, effectively providing virtual inertia and improved frequency stability. When a low-pass filter (LPF) is introduced in the droop path, the resulting LPF-based droop exhibits a first-order dynamic lag that produces a RoCoF-proportional component in the transient power response. Under the small-signal assumption, the LPF-based droop and the linearized VSM dynamics become mathematically equivalent by mapping the parameters as $D = 1/m_p$ and $J = \tau/m_p$ (equivalently, $J = D\tau$), which is consistent with the relationship shown in Fig. 9. This equivalence is also captured by (4), repeated below, indicating that both controllers can achieve identical closed-loop performance when the parameters are matched:

$$\Delta f = m_p \cdot \frac{1}{1 + s\tau} \Delta P = \frac{1}{D + sJ} \Delta P. \tag{4}$$

Accordingly, the simulation results confirm that the LPF-based droop, with properly mapped parameters, yields transient response and damping performance comparable to the VSM controller for weak-grid frequency-support applications.

IV. Conclusion

This paper demonstrated the technical maturity of domestically developed HVDC technology through the design, construction, and commissioning process of the ±120 kV 200 MW Yangju BTB MMC-HVDC system and introduced the Seohaean Energy Highway initiative currently promoted by the Korean government, as well as Hyosung Heavy Industries' development plan to complete a ±525 kV 2 GW HVDC system by 2027. In particular, the GFM–based HVDC simulation model was developed and verified to confirm its capability to enhance system stability and support renewable power transmission under weak-grid conditions. Future work will focus on hardware-in-the-loop (HILS) testing using a real controller equipped with GFM-based bi-pole control, protection, and operational algorithms. These continued developments will contribute to Korea's energy transition toward a resilient, renewable-based power system.

References

[1] J. Matevosyan, B. Badrzadeh, T. Prevost, E. Quitmann, D. Ramasubramanian, H. Urdal, S. Achilles, J. MacDowell, S. H. Huang, V. Vital, J. O'Sullivan, and R. Quint, "Grid-forming inverters: Are they the key for high renewable penetration?" *IEEE Power and Energy Magazine*, vol. 17, no. 6, pp. 89–98, 2019.

[2] K. Shinoda, P. Torwelle, and P. Verrax, "Grid-forming functional requirements for HVDC converter stations and dc-connected power park modules in multi-terminal multi-vendor HVDC systems," InterOPERA Consortium, Deliverable 2.2, Jan 2024.

[3] Ministry of Trade, Industry and Energy (MOTIE), "The 11th basic plan for long-term electricity supply and demand (2024–2038)," Government of Korea, Tech. Rep., 2024.

[4] H. W. Lee, D. S. Hyun, and J. H. Kim, "A study on the optimal operating point selection of the yangju 200 mw btb vsc-hvdc system," *The Transactions of the Korean Institute of Electrical Engineers (P Section)*, vol. 72, no. 4, pp. 326–330, 2023.

[5] P. Sun, Y. Tian, J. Pou, and G. Konstantinou, "Beyond the MMC: Extended modular multilevel converter topologies and applications," *IEEE Open Journal of Power Electronics*, vol. 3, pp. 317–333, 2022.

[6] North American Electric Reliability Corporation (NERC), "White paper: Grid forming functional specifications for BPS-connected battery energy storage systems," North American Electric Reliability Corporation, White Paper, Sep 2023.

[7] R. Rosso, X. Wang, M. Liserre, X. Lu, and S. Engelken, "Grid-forming converters: Control approaches, grid-synchronization, and future trends—a review," *IEEE Open Journal of Industry Applications*, vol. 2, pp. 93–109, 2021.

[8] R. Ofir, U. Markovic, P. Aristidou, and G. Hug, "Droop vs. virtual inertia: Comparison from the perspective of converter operation mode," in *2018 IEEE International Energy Conference (ENERGYCON)*, 2018, pp. 108–113.

979-8-3315-8138-1